Supplementary Figures and Legends

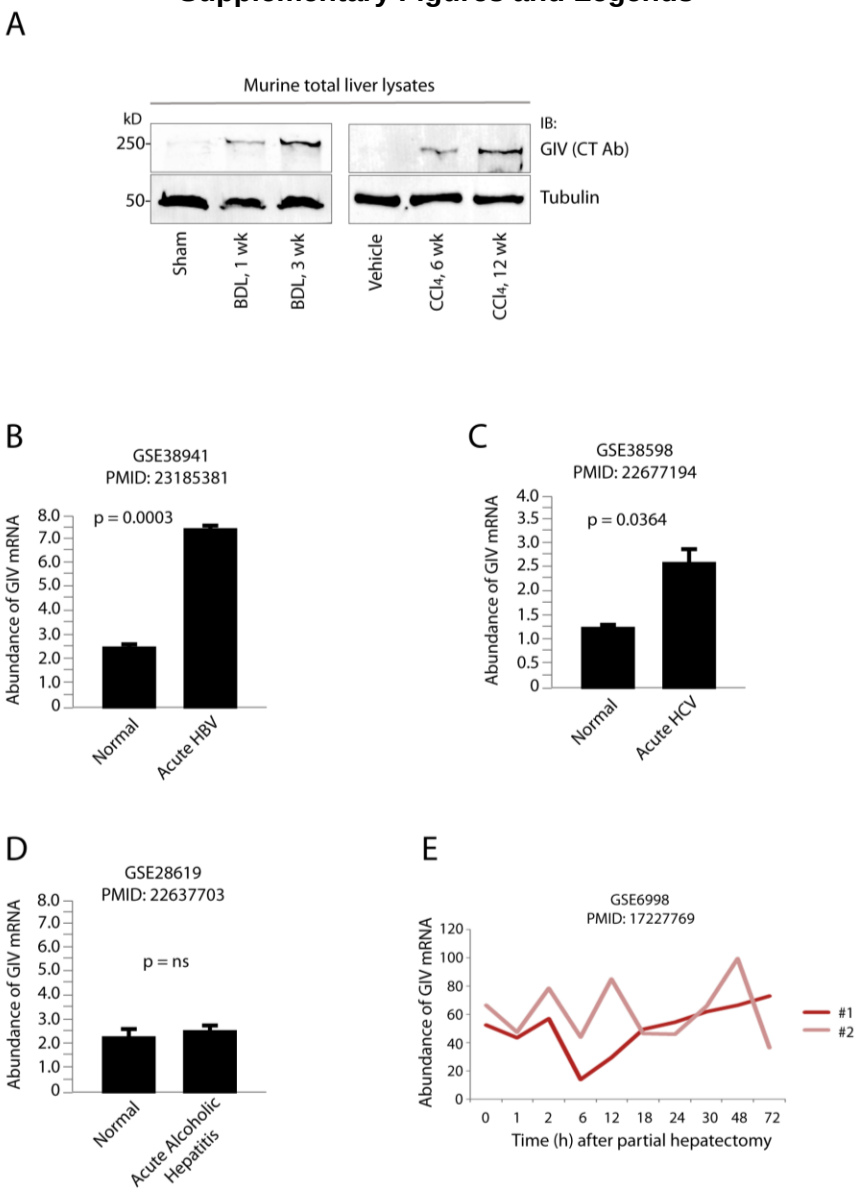

Supplementary Fig. 1. **Changes in GIV expression after liver injury.** (**A**) Equal aliquots of mouse liver lysates prepared from mice undergoing sham or BDL surgeries (left) and chronic injection with vehicle or CCl_4 (right) were analyzed for full length GIV and tubulin by immunoblotting. GIV is expressed exclusively after both forms of chronic injuries. Maximal GIV expression is seen at 3 wk after BDL and 12 wk of CCl_4 injuries coinciding with the development of overt cirrhosis. n = 3. (**B-E**) **Changes in GIV mRNA expression after acute liver injuries.** Expression of GIV mRNA is minimally, but significantly induced after injuries like hepatitis due to HBV (**B**) or HCV (**C**) infections, but not in acute alcoholic hepatitis (**D**) or after partial hepatectomy (**E**). Publicly available microarray datasets were mined for expression profile of GIV (gene name: ccdc88a) in various pathological conditions of the liver. (**B**) Bar graphs display the abundance of GIV mRNA expression in liver samples derived from patients with liver failure due to acute HBV infection (n = 4; 4-5 samples per liver) and normal livers (n=10; donor livers) as assessed by microarray in a previously published work [1]. (**C**) Bar graphs display the abundance of GIV mRNA expression in liver samples derived from patients with acute HCV monoinfection (n = 6, all within 2-5 mo of contracting HCV infection) and normal livers (n = 4) as assessed by microarray in a previously published work [2]. (**D**) Bar graphs display the abundance of GIV mRNA expression in liver samples derived from patients with alcoholic hepatitis (n=15) and normal livers (n=7) as assessed by microarray in a previously published work [3]. Hybridizations in B were done on GeneChip Mouse Genome 430 2.0 Array, whereas C-E were done on [HG-U133_Plus_2] Affymetrix Human Genome U133 Plus 2.0 Arrays. (**E**) Linear graphs display the abundance of GIV mRNA expression in liver samples derived from 10-week-old normal female mice at indicated time points after partial (2/3 rd) hepatectomy as assessed by microarray in previously published work [4]. Error bars represent mean ± S.D.

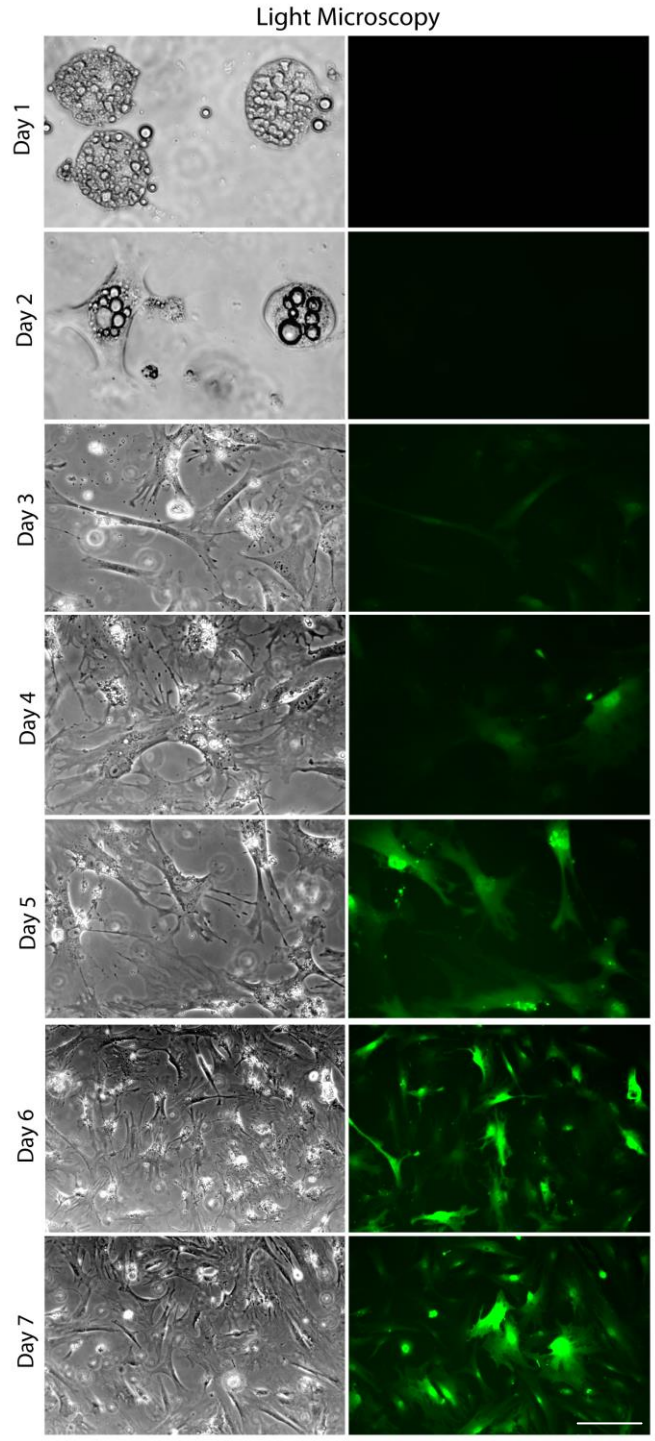

Supplementary Fig. 2. Activation of primary murine HSCs isolated from livers of Col-GFP mice in culture. HSCs were isolated from Col-GFP mice and cultured on tissue culture dishes for 7 days. Cellular morphology (left) and GFP expression (right; surrogate marker of collagen production) were monitored simultaneously using light microscopy. Representative images on different days are shown. Inactive HSCs show abundance of retinoid droplets on days 1 and 2, and activation was characterized by loss of retinoid droplets and increased collagen production (as seen on day 3), as determined by a progressive gain of GFP signal intensity (right). Scale bar = 200 µm.

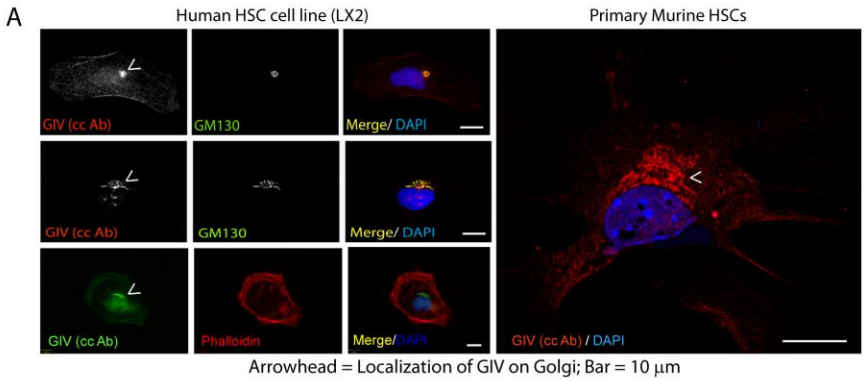

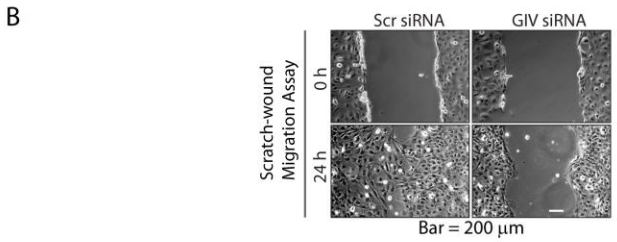

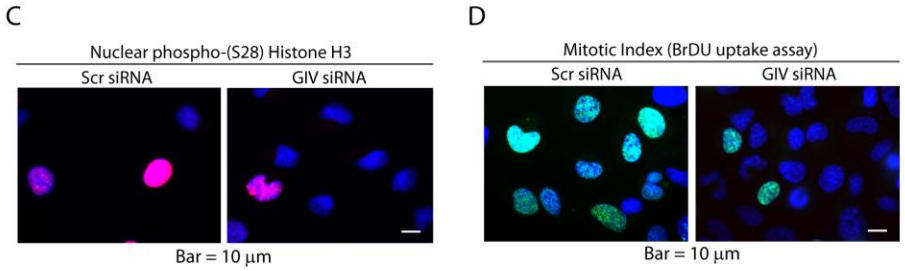

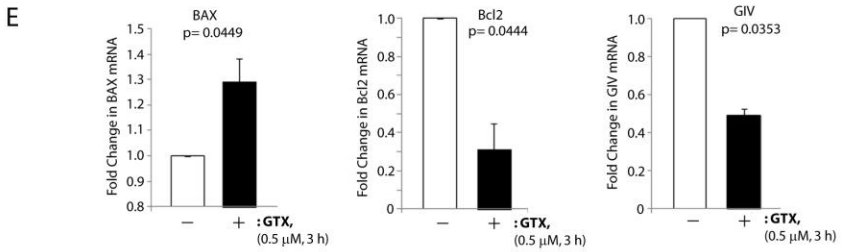

Supplementary Fig. 3. Characterization of GIV's localization and functions in Lx2 cells. (**A**) GIV localizes at the Golgi complex and in actin fibers in hepatic stellate cells as previously described for other cell lines [5,6]. Lx2 cells and primary murine HSCs were fixed and stained for GIV (red or green), GM130 (Golgi marker, green), phalloidin-Texas Red (F- actin, red) and DAPI/DNA (blue) and analyzed by confocal microscopy. GIV on the Golgi apparatus is indicated by arrowheads. Scale bar = 10 μm. (**B**) Depletion of GIV impairs Lx2 cell migration in scratch wound assays. Cells were either treated with control (Scr) or with GIV siRNA for 36 h, grown to 100% confluency, scratch-wounded, and serial images were taken by phase-contrast microscopy over the next 24 h. Images of representative fields are shown. Scale bar = 200 μm. Bar graph in Figure **4D** shows the quantification of the percentage of wound area closed by 24 h. Cells depleted of GIV are unable to close the wound compared to control cells. (**C** and **D**) Depletion of GIV impairs Lx2 cell proliferation. Cells were either treated with control (Scr) or with GIV siRNA, fixed and costained with anti-phospho-Histone H3 (Ser28) antibody (red) (**C**) or anti-BrDU antibody (green) (**D**) and DAPI/DNA (blue). Images were analyzed by confocal microscopy and images of representative fields are shown. Scale bar = 10 μm. Mitotic index was calculated as a percentage of the number of cells positive for phospho-Histone H3 or BrDU compared to the total of cell number with DAPI-stained nuclei. Quantifications are shown in **Figure 4E** and **4F**. (**E**) Apoptosis was induced in Lx2 cells with Gliotoxin (GTX), and cells were analyzed for BAX, Bcl-2 and GIV mRNA by qPCR. Pro-apoptotic BAX is upregulated (left), but anti-apoptotic Bcl-2 is downregulated (middle). GIV is downregulated much like anti-apoptotic intermediate Bcl-2 (right). Results are displayed as fold change compared to the vehicle-treated control. Error bars represent mean ± S.D. Statistical significance was assessed with two-tailed Student's t-test.

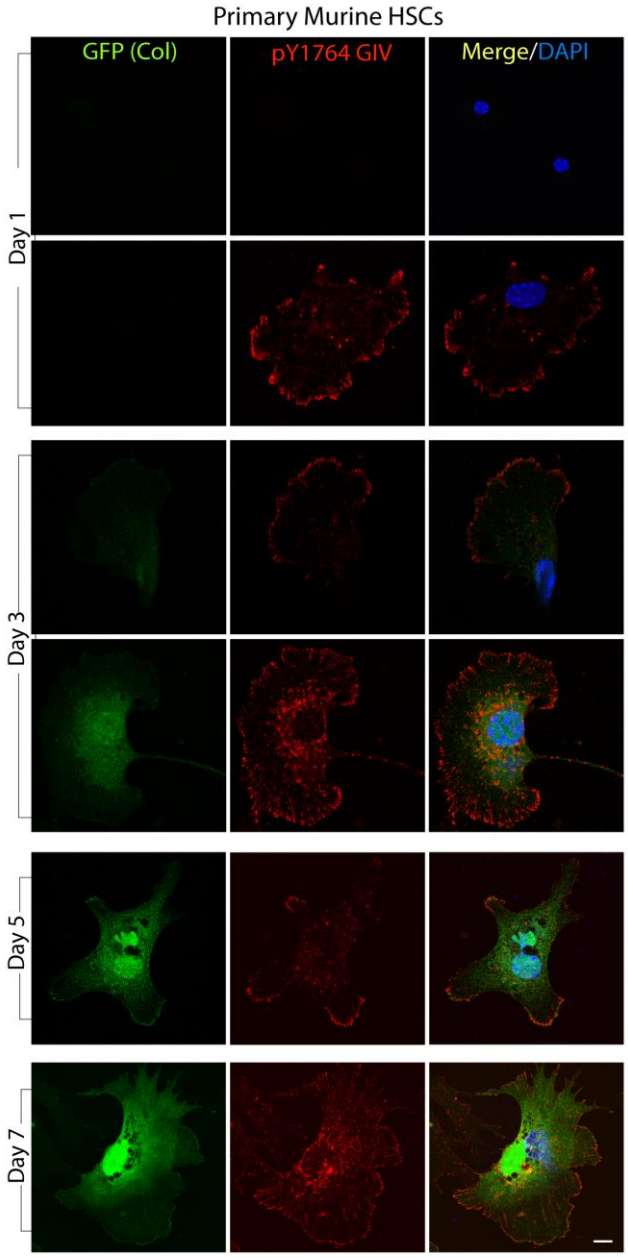

Supplementary Fig. 4. Activation of the RTK-GIV-PI3K pathway, as determined by the extent of tyrosine phosphorylation of GIV as a surrogate marker precedes collagen production in culture-activated HSCs. Primary HSCs isolated from Col-GFP mice were activated in culture for 7 days. Cells were fixed for immunofluorescence at various time points and stained for active GIV (red, pY1764-GIV) and DAPI/DNA (blue) and analyzed by confocal microscopy. Collagen production was detected by GFP signal. Scale bar = 10 μm.

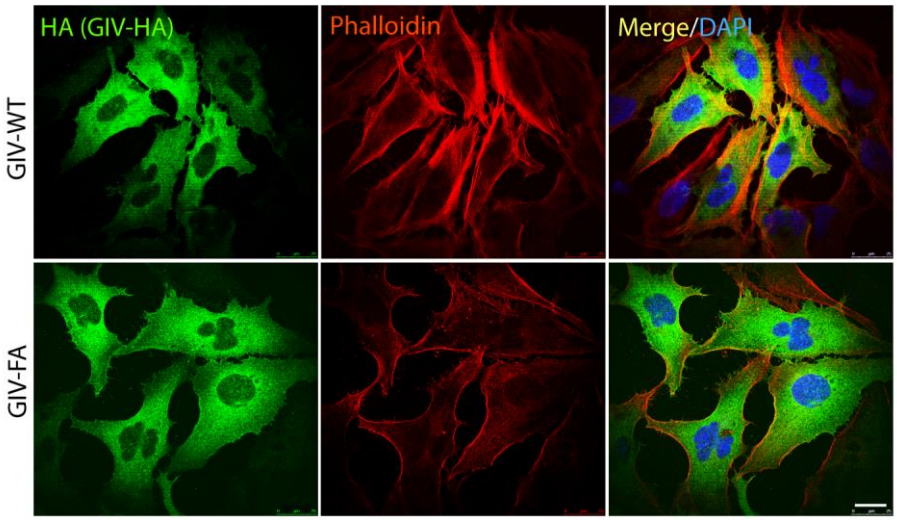

Supplementary Fig. 5. GIV´s GEF function is required for actin stress fibers formation. Lx2 cells infected with GIV-WT-HA or GIV-FA-HA adenoviruses were maintained in 0.2% FBS, fixed and stained for HA (GIV, green), Phalloidin (red) and DAPI/DNA (blue) and analyzed by confocal microscopy. Cells expressing GIV-WT show abundance of actin stress fibers, whereas cells expressing GEF-deficient GIV shows paucity of stress fibers. Scale bar = 10 µm..

FIGURE 4A.

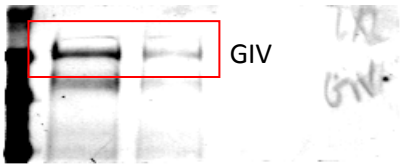

FIGURE 7C and 6B.

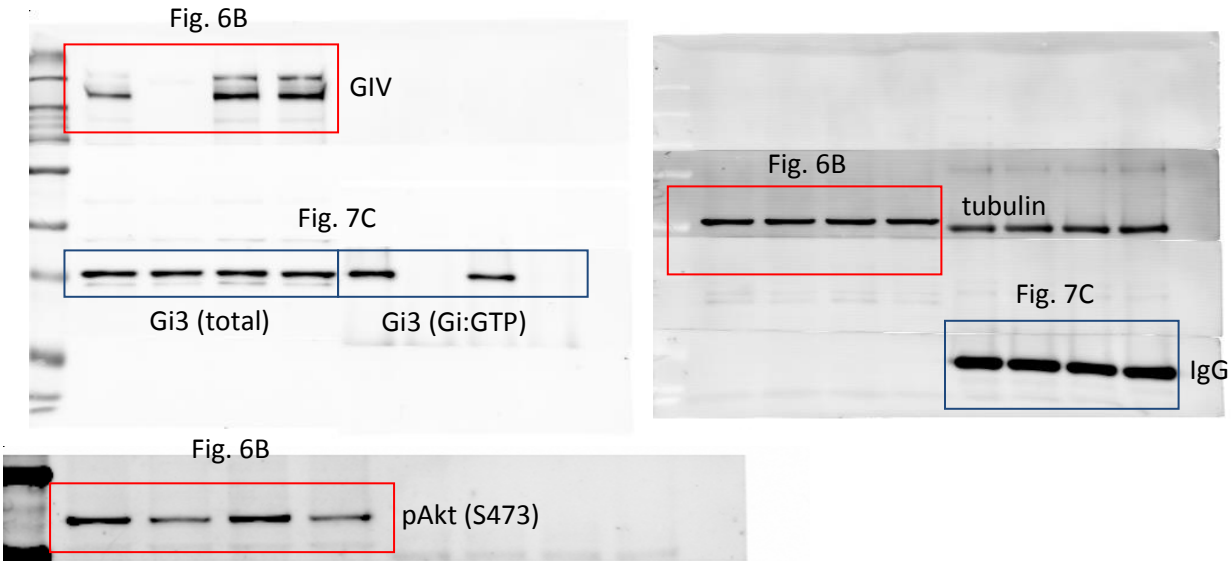

Supplementary Fig. 6. Raw LiCOR Odyssey image files of the key figures. Boxes indicate the portions used in the figures, and the numbers indicate the corresponding figure panels in the manuscript.

FIGURE 6D.

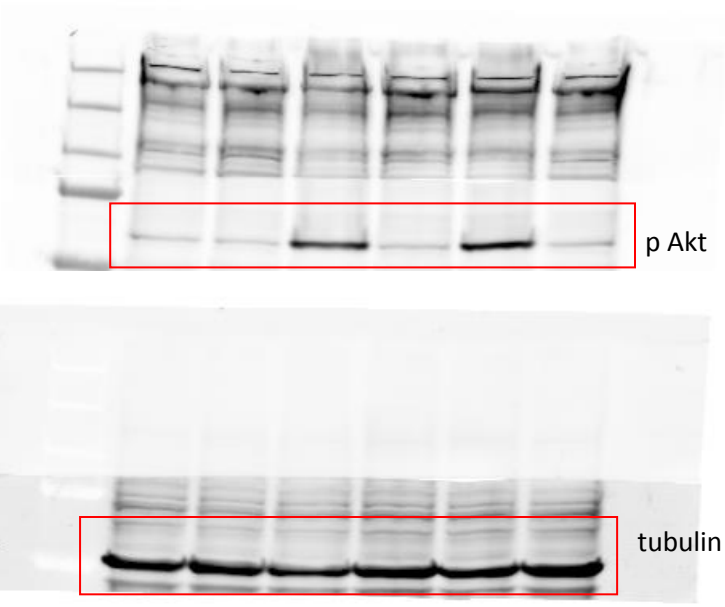

FIGURE 6K.

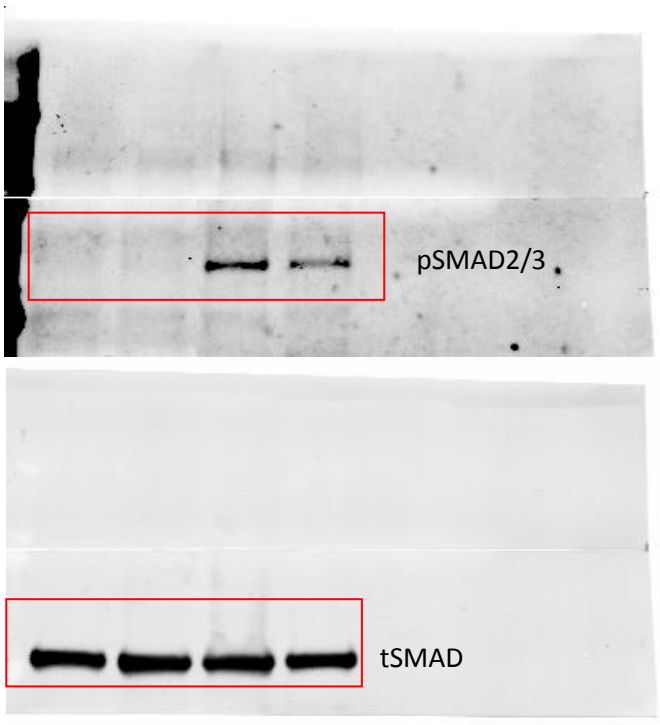

Supplementary Fig. 7. Raw LiCOR Odyssey image files of the key figures. Boxes indicate the portions used in the figures, and the numbers indicate the corresponding figure panels in the manuscript.

FIGURE 7B.

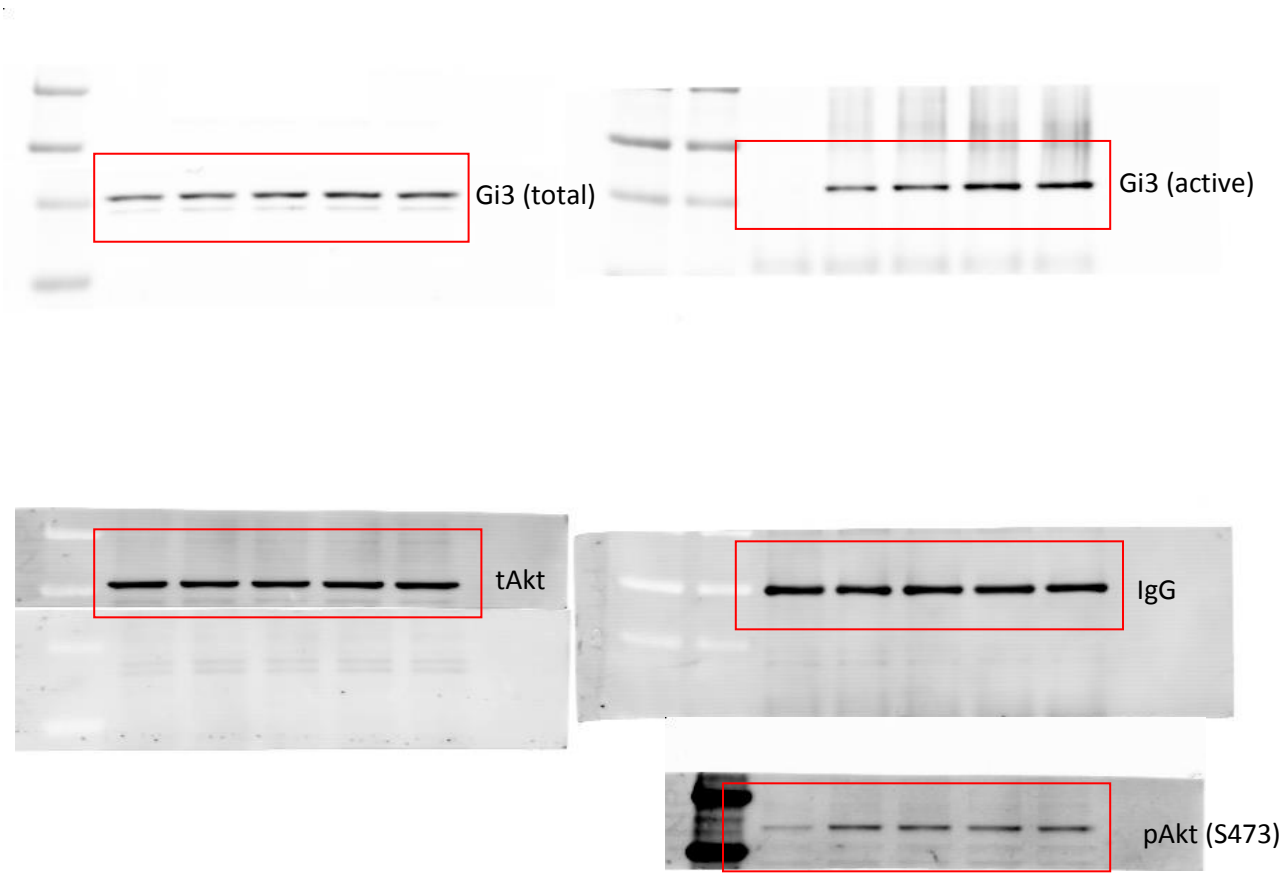

Supplementary Fig. 8. Raw LiCOR Odyssey image files of the key figures. Boxes indicate the portions used in the figures, and the numbers indicate the corresponding figure panels in the manuscript.

FIGURE 7E.

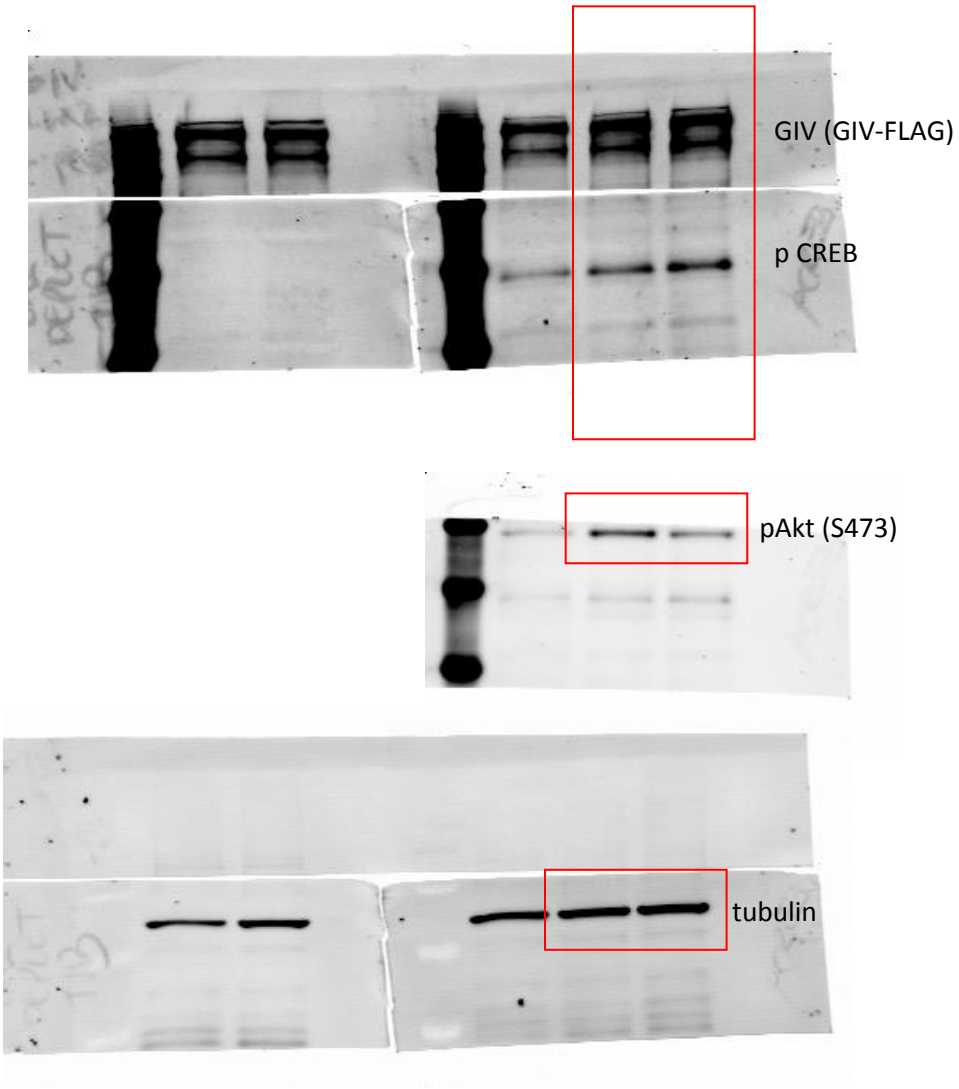

Supplementary Fig. 9. Raw LiCOR Odyssey image files of the key figures. Boxes indicate the portions used in the figures, and the numbers indicate the corresponding figure panels in the manuscript.

Supplementary Table 1. Primers used for *quantitative PCR (qPCR).*

Gene/Protein	Forward	Reverse
Cddc88a/m-hGIV	5´-GTGATCTCTACTGCTGAAGG-3´	5´-CCTAGACCTGCTTTTTGAATTTCT-3´
Col1a1/hCollagen	5´-TCTACTGGCGAAACCTGTATCCG-3´	5´-CAAGGAAGGGCAGGCGTGAT-3´
Col1a1/mCollagen	5´-TAGGCCATTGTGTATGCAGC-3´	5´-ACATGTTCAGCTTTGTGGACC-3´
Acta2/α-SMA	5´-GTTCAGTGGTGCCTCTGTCA-3	5´-ACTGGGACGACATGGAAAAG-3´
Bax/BAX	5´-TGGAGCTGCAGAGGATGATTG-3´	5´-GAAGTTGCCGTCAGAAAACATG-3´
Bcl-2/BCL-2	5´- GTTGGTGGGGTCATGTGTGTGGAGAG-3´	5´-TAGCTGATTCGACGTTTTGCCTGA-3´
Gapdh/hGAPDH	5'- TCAGTTGTAGGCAAGCTGCGACGT-3'	5'-AAGCCAGAGGCTGGTACCTAGAAC-3´
Gapdh/mGAPDH	5´-TGTGTCCGTCGTGGATCTGA-3´	5´-TTGCTGTTGAAGTCGCAGGAG-3´

Supplementary References

1 Nissim, O. *et al.* Liver regeneration signature in hepatitis B virus (HBV)-associated acute liver failure identified by gene expression profiling. *PloS one* **7**, e49611, doi:10.1371/journal.pone.0049611 (2012).

2 Dill, M. T. *et al.* Interferon-gamma-stimulated genes, but not USP18, are expressed in livers of patients with acute hepatitis C. *Gastroenterology* **143**, 777-786 e771-776, doi:10.1053/j.gastro.2012.05.044 (2012).

3 Affo, S. *et al.* Transcriptome analysis identifies TNF superfamily receptors as potential therapeutic targets in alcoholic hepatitis. *Gut* **62**, 452-460, doi:10.1136/gutjnl-2011-301146 (2013).

4 Otu, H. H. *et al.* Restoration of liver mass after injury requires proliferative and not embryonic transcriptional patterns. *The Journal of biological chemistry* **282**, 11197-11204, doi:10.1074/jbc.M608441200 (2007).

5 Le-Niculescu, H., Niesman, I., Fischer, T., DeVries, L. & Farquhar, M. G. Identification and characterization of GIV, a novel Galpha i/s-interacting protein found on COPI, endoplasmic reticulum-Golgi transport vesicles. *The Journal of biological chemistry* **280**, 22012-22020, doi:10.1074/jbc.M501833200 (2005).

6 Jiang, P. *et al.* An actin-binding protein Girdin regulates the motility of breast cancer cells. *Cancer research* **68**, 1310-1318 (2008).